

Laboratori Nazionali di Frascati

Submitted to Phys. Lett. B

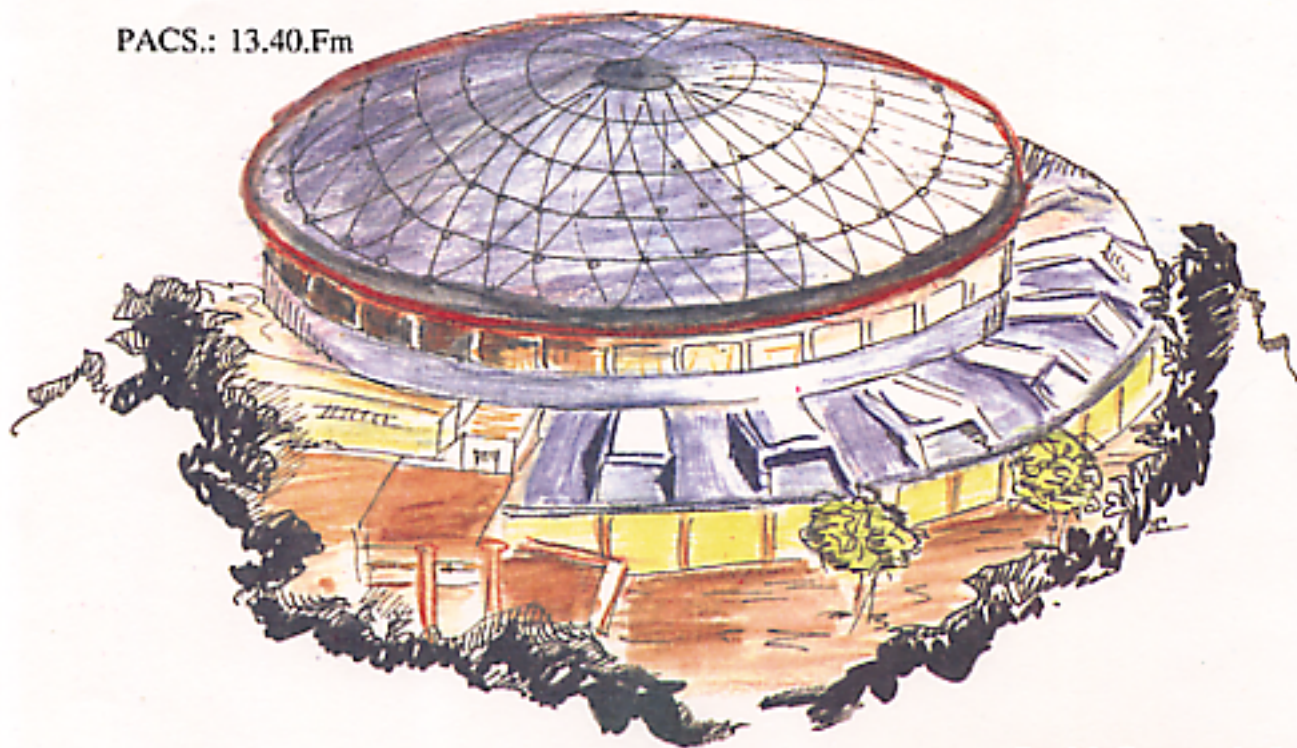
LNF-94/032 (P)

14 Giugno 1994

A. Antonelli, R. Baldini, M. Bertani, M.E. Biagini, V. Bidoli, C. Bini, T. Bressani, R. Calabrese, R. Cardarelli, R. Carlin, C. Casari, L. Cugusi, P. Dalpiaz, A. De Falco, G. De Zorzi, A. Feliciello, M.L. Ferrer, P. Ferretti, P. Gauzzi, P. Gianotti, E. Luppi, S. Marcello, A. Masoni, R. Messi, M. Morandin, L. Paoluzi, E. Pasqualucci, G. Pauli, N. Perlotto, F. Petrucci, M. Posocco, G. Puddu, M. Reale, L. Santi, R. Santonico, P. Sartori, M. Savriè, S. Serci, M. Spinetti, S. Tessaro, C. Voci, F. Zuin:

**MEASUREMENT OF THE ELECTROMAGNETIC FORM FACTOR
OF THE PROTON IN THE TIME-LIKE REGION**

PACS.: 13.40.Fm



**MEASUREMENT OF THE ELECTROMAGNETIC FORM FACTOR OF THE
PROTON IN THE TIME-LIKE REGION**

A. Antonelli⁽³⁾, R. Baldini⁽³⁾, M. Bertani⁽³⁾, M. E. Biagini⁽³⁾, V. Bidoli⁽⁶⁾, C. Bini⁽⁵⁾,
T. Bressani⁽⁷⁾, R. Calabrese⁽²⁾, R. Cardarelli⁽⁶⁾, R. Carlin⁽⁴⁾, C. Casari⁽¹⁾, L. Cugusi⁽¹⁾,
P. Dalpiaz⁽²⁾, A. De Falco⁽¹⁾, G. De Zorzi⁽⁵⁾, A. Feliciello⁽⁷⁾, M. L. Ferrer⁽³⁾,
P. Ferretti⁽²⁾, P. Gauzzi⁽⁵⁾, P. Gianotti⁽⁷⁾, E. Luppi⁽²⁾, S. Marcello⁽⁷⁾, A. Masoni⁽¹⁾,
R. Messi⁽⁶⁾, M. Morandin⁽⁴⁾, L. Paoluzi⁽⁶⁾, E. Pasqualucci⁽⁶⁾, G. Pauli⁽⁸⁾, N. Perlotto⁽⁴⁾,
F. Petrucci⁽²⁾, M. Posocco⁽⁴⁾, G. Puddu⁽¹⁾, M. Reale⁽⁶⁾, L. Santi⁽⁹⁾, R. Santonico⁽⁶⁾,
P. Sartori⁽⁴⁾, M. Savriè⁽²⁾, S. Serci⁽¹⁾, M. Spinetti⁽³⁾, S. Tessaro⁽⁸⁾, C. Voci⁽⁴⁾, F. Zuin⁽⁴⁾

(1) Dipartimento di Fisica dell'Università and INFN, Cagliari

(2) Dipartimento di Fisica dell'Università and INFN, Ferrara

(3) INFN Laboratori Nazionali di Frascati

(4) Dipartimento di Fisica dell'Università and INFN, Padova

(5) Dipartimento di Fisica dell'Università and INFN, Roma "La Sapienza"

(6) Dipartimento di Fisica dell'Università and INFN, Roma "Tor Vergata"

(7) Dipartimento di Fisica dell'Università and INFN, Torino

(8) Dipartimento di Fisica dell'Università and INFN, Trieste

(9) Dipartimento di Fisica dell'Università di Udine and INFN Trieste

Abstract.

The cross section for the process $e^+e^- \rightarrow p\bar{p}$ has been measured in the s range $3.6 \div 5.9 \text{ GeV}^2$ by the FENICE experiment at the e^+e^- Adone storage ring and the proton electromagnetic form factor has been extracted.

1. Introduction

The proton electromagnetic form factors have been widely investigated in the space-like region by means of elastic scattering of electrons on hydrogen targets [1]. Several measurements have been performed also in the time-like region at s values between the nucleon-antinucleon threshold ($s = (2M_p)^2 = 3.52 \text{ GeV}^2$) and $s = 13 \text{ GeV}^2$, exploiting two different experimental techniques: the detection of the process $e^+e^- \rightarrow p\bar{p}$ at e^+e^- storage rings [2] and the process $p\bar{p} \rightarrow e^+e^-$ by means of antiproton annihilation on a hydrogen target [3,4,5]. As well as in the space-like region, but approaching a different proportionality constant value, a $1/s^2$ asymptotic behaviour is experimentally found for the magnetic form factor $|G_M^p|$, in agreement with what is expected on the basis of dimensional arguments [6]. In the s range from threshold up to $\sim 4 \text{ GeV}^2$, the most recent results show a steep slope of the form factor just above threshold. Furthermore, the first measurements of the neutron time-like form factor [7] near threshold give a hint for a neutron form factor being larger or equal than the proton one in contrast with simple QCD based arguments [8].

In this paper more data on the proton time-like form factor from the FENICE experiment at the Adone e^+e^- storage ring are presented.

2. Experimental apparatus

Adone was an e^+e^- storage ring operating at center of mass energies in the range $1.5 < \sqrt{s} < 3.1 \text{ GeV}$ with a mean luminosity of $10^{29} \text{ cm}^{-2}\text{s}^{-1}$, the uncertainty on the absolute value of the center of mass energy being about $\pm 5 \text{ MeV}$.

The FENICE detector [9] has been designed mainly for the measurement of the process $e^+e^- \rightarrow n\bar{n}$ from threshold up to the J/ψ resonance energy [10], but the detection of other final states is also possible. It is a non-magnetic detector with a solid angle coverage of $0.76 \times 4\pi \text{ sr}$. A Central Detector (CD), consisting of a layer of 0.5 cm thick scintillators and 4 planes of Limited Streamer Tubes (LST) [11], surrounds the $300 \mu\text{m}$ thick iron wall of the beam pipe. The antinucleon detector designed for the detection of the multi-track topologies of \bar{n} or \bar{p} annihilations on nuclei consists of alternate layers of 0.5 cm thick iron plates, 2 or 5 cm thick scintillator slabs and LST planes. The expected average numbers of charged and neutral pions in the detector are 2.3 and 1.5 respectively. The scintillators are employed for triggering and for time of flight (TOF) measurements, the LST planes for tracking. The TOF resolution is about 600 ps per scintillator, taking into account the beam crossing time spread. Finally an array of Resistive Plate Counters (RPC) [12] used in anticoincidence in the trigger, surrounds a concrete hut, built around the detector in order to reduce the rate of cosmic rays interacting in the detector.

3. Data analysis and results

The FENICE experiment took data at center of mass energies $\sqrt{s} = 1.9, 1.92, 2.0, 2.1$ and 2.44 GeV ; special runs have been done just below the nucleon-antinucleon

threshold from $\sqrt{s} = 1.82 \text{ GeV}$ to 1.86 GeV in order to evaluate the residual background. The primary goal of the experiment was the first measurement of the neutron time-like form factor. However the detection of $p\bar{p}$ events allowed the measurement of the proton form factor too. A preliminary result on the proton form factor at $s = 4.4 \text{ GeV}^2$ has already been reported [7]. In this paper further results on the proton form factor at different s are given.

The event selection proceeds in three steps:

- (1) the raw data are filtered in order to reject cosmic rays, beam-gas interactions background and collinear two-tracks events (e^+e^- , $\mu^+\mu^-$ and $\gamma\gamma$) with no appreciable loss of efficiency. At this stage multi-hadronic events are identified and rejected;
- (2) $p\bar{p}$ candidates are selected asking for two aligned tracks in the CD. At $\sqrt{s} \leq 1.92 \text{ GeV}$ a track is defined by a hit in the CD scintillator, while at higher \sqrt{s} it is defined by a sequence of at least 3 hits out of the 4 planes of LST in the CD. The collinearity request ranges from $\pm 18^\circ$ (fixed by the scintillator width) at $\sqrt{s} = 1.92 \text{ GeV}$ and $\pm 10^\circ$ at higher \sqrt{s} .
- (3) finally the signature of $p\bar{p}$ events is the coincidence of an annihilation star originated by a charged particle (\bar{p} signal) and a track back to back the annihilation star (p signal). At $\sqrt{s} \leq 1.92 \text{ GeV}$ both p and \bar{p} stop in the CD scintillator layer and the \bar{p} annihilates at rest. On the contrary, at $\sqrt{s} \geq 2.0 \text{ GeV}$ both particles penetrate deeper into the detector and the \bar{p} can annihilate also in flight with a probability ranging from 10% at 2.0 GeV to 65% at 2.44 GeV . The final samples of events are visually scanned to reject residual events with topologies not compatible with $p\bar{p}$ events.

In the samples of events that survive the selection procedure, residual background events could be beam-gas or beam-pipe interactions and multi-hadronic events simulating annihilation stars. Both background sources are more relevant when the \bar{p} annihilates closer to the interaction region. A discriminant feature between these background events and the $p\bar{p}$ events is the time of flight, since both the p and the \bar{p} are characterized by $0.16 < \beta < 0.64$ in the explored s region. At $\sqrt{s} \geq 2.0 \text{ GeV}$ a measurement of $\beta_{\bar{p}}$ is provided by vertex reconstruction and by TOF measurement in the scintillators closer to the vertex region. At $\sqrt{s} \leq 1.92 \text{ GeV}$ such a measurement is not possible due to the very short path of the outgoing \bar{p} . In this case the average time of flight of the event \bar{T} is used as discriminant variable.

In Fig.1 the \bar{T} distributions are shown for the selected samples below threshold (Fig.1a) and at $\sqrt{s} = 1.92 \text{ GeV}$ (Fig.1b). The excess of events at high \bar{T} observed in the second sample corresponds to the expected $p\bar{p}$ signal. A cut at 4.8 ns is suggested by comparing the distributions shown with the Montecarlo simulation. An excess of events separated from residual background is observed also at $\sqrt{s} = 1.90 \text{ GeV}$. However, due to the uncertainty on the absolute value of the center of mass energy, the systematic error on the selection efficiency evaluation is very large and does not allow us to estimate reliably the form factor $|G^p|^1$.

In Fig.2 the $1/\beta_{\bar{p}}$ distribution of the selected events at $\sqrt{s} = 2.1 \text{ GeV}$ is shown.

¹Antineutrons have a longer mean path hence the TOF measurement of antineutrons from $e^+e^- \rightarrow n\bar{n}$ will allow to reduce this uncertainty.

Table 1:

$s(\text{GeV}^2)$	$\mathcal{L} (\text{nb}^{-1})$	$\epsilon_{p\bar{p}}$	$N_{p\bar{p}}$	$\sigma(e^+e^- \rightarrow p\bar{p}) (\text{nb})$	$ G^p $
3.69	79.6 ± 4.8	0.21 ± 0.02	16 ± 4.5	$0.96 \pm 0.25 \pm 0.11$	$0.36 \pm 0.05 \pm 0.02$
4.00	93.9 ± 5.6	0.31 ± 0.03	18 ± 4.7	$0.62 \pm 0.16 \pm 0.06$	$0.24 \pm 0.03 \pm 0.01$
4.41	99.9 ± 6.0	0.45 ± 0.03	28 ± 5.3	$0.62 \pm 0.11 \pm 0.05$	$0.22 \pm 0.02 \pm 0.01$
5.95	57.1 ± 3.4	0.44 ± 0.031	7 ± 2.6	$0.28 \pm 0.11 \pm 0.05$	$0.15 \pm 0.03 \pm 0.01$

The distribution is compatible with a gaussian one, centered at the expected value: the residual small background is subtracted in the calculation of the final number of events.

Simulation of $p\bar{p}$ events in the detector has been done taking into account radiative corrections on the initial state [13] which considerably affect the efficiency evaluation; \bar{p} annihilation cross-sections are taken from [14] and pions are generated according to invariant phase-space. The detection efficiency is evaluated by submitting simulated events to the same selection procedure used for real data.

The luminosity is measured by means of Bhabha scattering in the FENICE detector and is checked with $\mu^+\mu^-$ and $\gamma\gamma$ rates. An external fast luminosity monitor based on the detection of single bremsstrahlung photons [15] was also operating, giving luminosity values in agreement within 6% with the Bhabha measurement. The systematic error on the integrated luminosity is estimated to be $\pm 6\%$ for all the s values.

Tab.1 reports integrated luminosity \mathcal{L} , efficiency $\epsilon_{p\bar{p}}$, final number of events $N_{p\bar{p}}$ together with cross section σ and form factor $|G^p|$ for data in the $3.69 \div 5.93 \text{ GeV}^2$ range. The form factor is extracted from the total cross section according to

$$\sigma = \frac{4\pi\alpha^2\beta}{3s} |G^p(s)|^2 \left[1 + \frac{2M_p^2}{s}\right]^2$$

where M_p is the proton mass, β is the proton velocity and $|G^p|$ is the form factor in the hypothesis that $|G_E^p| = |G_M^p|$ also at $s \neq 4M_p^2$.

The error on $N_{p\bar{p}}$ includes the effect of background subtraction. In Table 1 the statistical and the systematic errors respectively are quoted for the cross sections and the form factors. The main contribution on the systematic error is given by the uncertainty on annihilation cross sections, annihilation pion spectra, and by LST efficiency variations. An overall $\pm 10\%$ systematic error is obtained.

Finally in Fig.3 the FENICE results are compared with worldwide data on proton form factor in the time-like region.

Acknowledgements

We are indebted to the ADONE staff for reviving ADONE as a collider, and to S.De Simone, S.Guiducci, F.Iazzi, B.Minetti, M.Preger and L.Tecchio for their collaboration in the experiment

References

- [1] R.Hofstadter, Electron scattering and nuclear and nucleon structure, (W.A. Benjamin, 1963);
- [2] M.Castellano et al., Nuovo Cimento A14 (1973) 1;
G.Bassompierre et al., Phys.Lett. B64 (1976) 475;
B.Delcourt et al., Phys.Lett. B86 (1979) 395;
D.Bisello et al., Nucl.Phys.B224 (1983) 379;
- [3] M.Conversi et al., Nuovo Cimento 40 (1965) 690;
D.L.Hartill et al., Phys.Rev. 184 (1969) 1415;
C.Baglin et al., Phys.Lett. B163 (1985) 400
G.Bardin et al., Phys.Lett. B255 (1991) 149; Phys.Lett. B257 (1991) 514;
- [4] T.A.Armstrong et al., Phys.Rev.Lett. 70 (1992) 1212;
- [5] G.Bardin et al., Nucl.Phys. B411 (1994) 3;
- [6] S.J.Brodsky and G.R.Farrar, Phys.Rev. D11 (1975) 1309;
- [7] A.Antonelli et al., Phys.Lett. B313 (1993) 283;
- [8] V.L.Cernyak and I.R.Zhitnitsky, Nucl.Phys. B246 (1984) 52;
- [9] A.Antonelli et al., Nucl.Instr.and Meth. A337 (1993) 34;
- [10] A.Antonelli et al., Phys.Lett. B301 (1993) 317;
- [11] G.Battistoni et al., Nucl.Instr.and Meth. A292 (1979) 57;
- [12] R.Santonico and R.Cardarelli, Nucl.Instr.and Meth. 187 (1981) 377;
- [13] E.A.Kuraev and V.S.Fadin, Sov.Journ. of Nucl.Phys. 41 (1985) 466;
J.Haissinski LAL 89-50 (1989);
- [14] A.Bressan et al., Trieste Int. Note, INFN/TC-93/14;
- [15] H.C.Dejne et al., Nucl.Instr. and Meth. 116 (1974) 345;

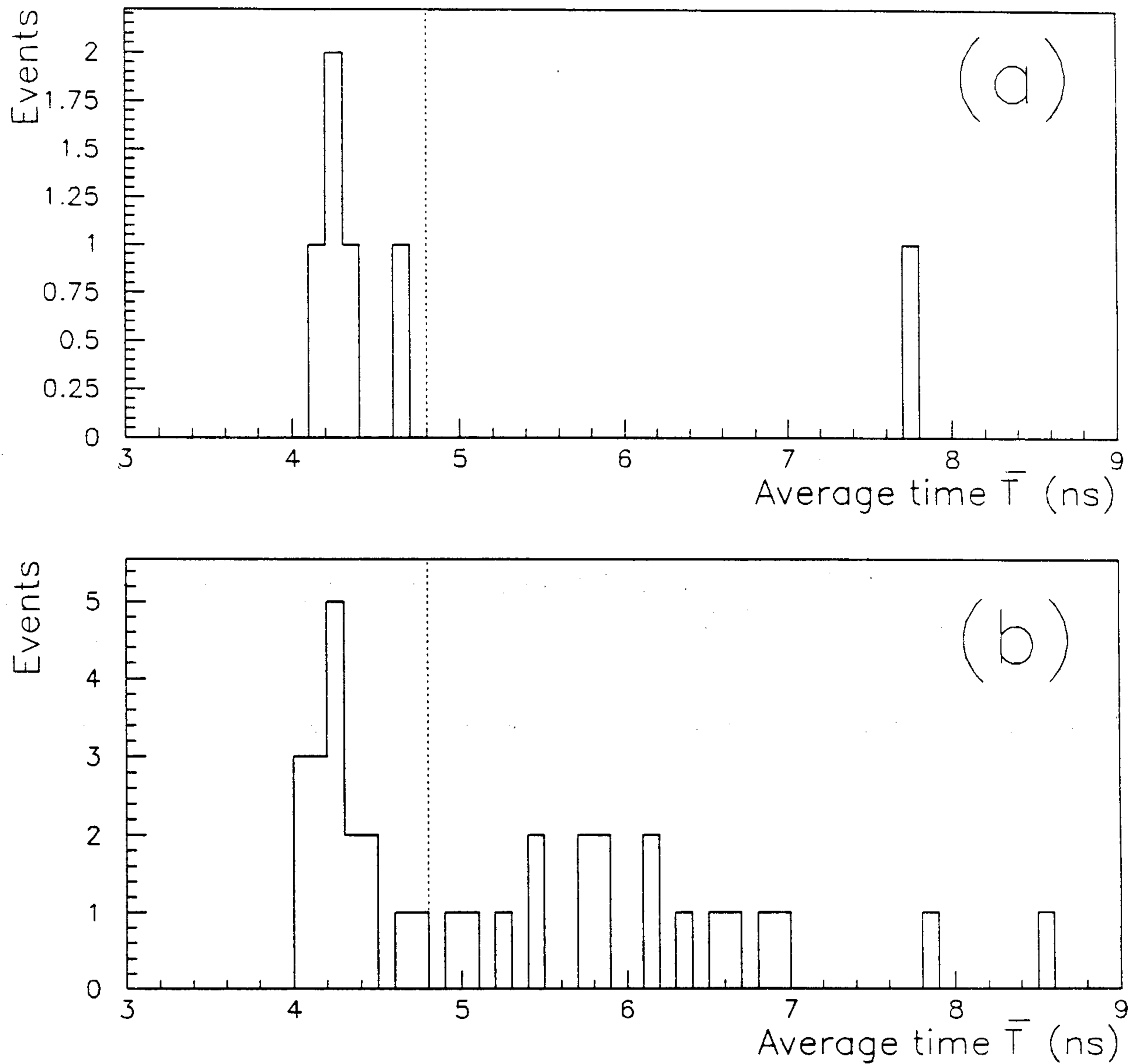


FIG. 1 – Average time \bar{T} distribution for events selected (a) below threshold $1.82 \geq \sqrt{s} \geq 1.86$ GeV and (b) at $\sqrt{s} = 1.92$ GeV. The $p\bar{p}$ signal at $\sqrt{s} = 1.92$ GeV is given by the number of events with $\bar{T} > 4.8$ ns (see dotted line).

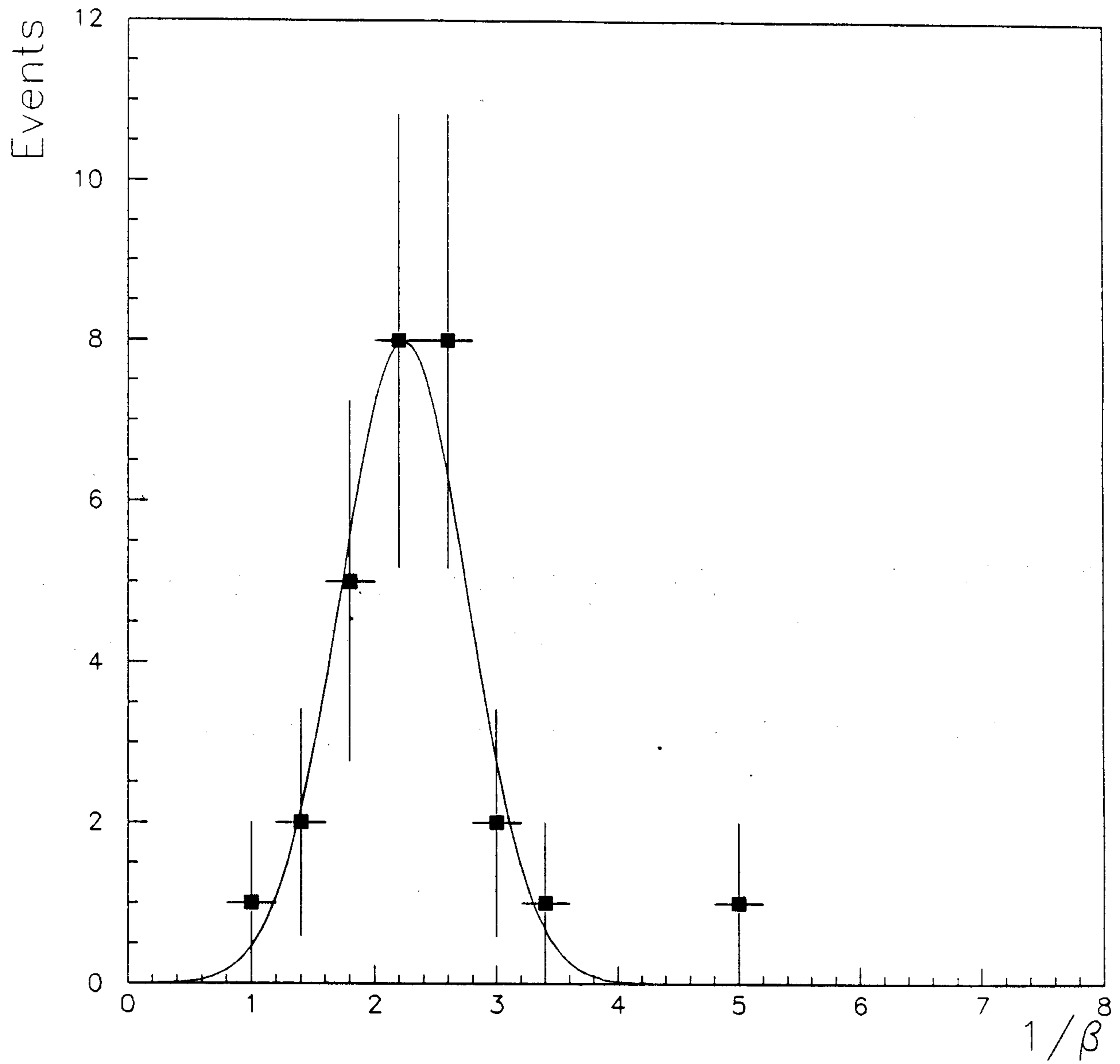


FIG. 2 - $1/\beta_p$ distribution for the candidate events at $\sqrt{s} = 2.1$ GeV.

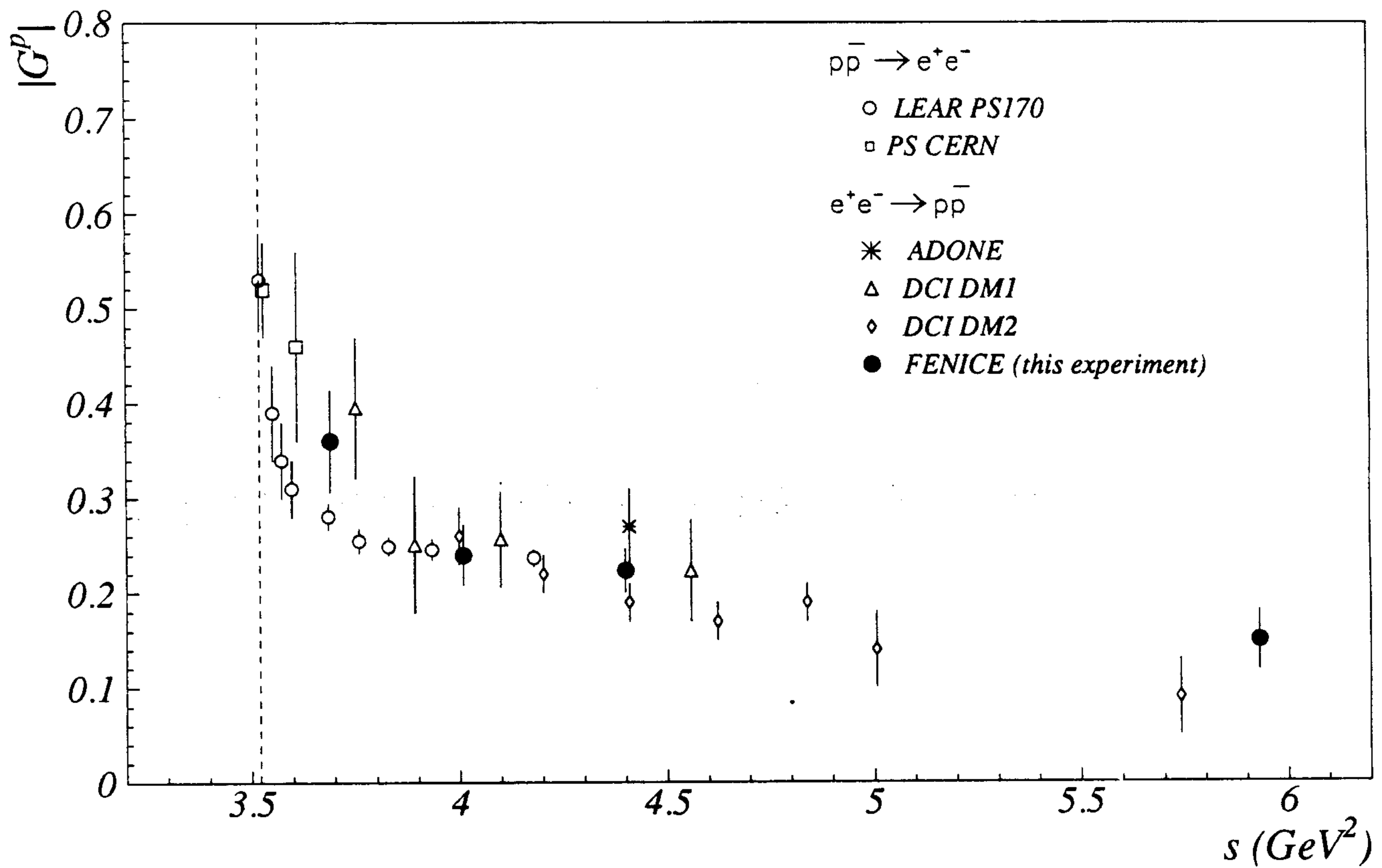


FIG. 3 – The proton electromagnetic form factor as a function of \sqrt{s} . The dashed line corresponds to the nucleon-antinucleon threshold. The FENICE results (full circles) are compared with worldwide data in the same s region.